Expert Systems with Applications 42 (2015) 527–538

Contents lists available at ScienceDirect

Expert Systems with Applications

journal homepage: www.elsevier.com/locate/eswa

Autonomous tracking of chemical plumes developed in both diffusive and turbulent airflow environments using Petri nets

Jie Yuan [a,b,*], David Oswald [b], Wei Li [c,b]

[a] School of Electrical Engineering, Xinjiang University, Urumqi Xinjiang 830047, China
[b] Department of Computer and Electrical Engineering, California State University, Bakersfield, CA 93311, USA
[c] Department of Electrical Engineering and Automation, Tianjin University, Tianjin 300072, China

ARTICLE INFO

Article history:
Available online 13 August 2014

Keywords:
Chemical plume tracing
Petri nets
Rule-based system
Diffusive and turbulent airflow
Knowledge

ABSTRACT

This paper presents a Petri net model for autonomous tracking of chemical plumes developed in both diffusive and turbulent airflow environments. It has been challenging to develop a generalized algorithm to effectively trace both types of chemical plumes due to the significant differences of their kinetic and dynamic properties. Our idea is to utilize a Petri net to model the change relationships of chemical concentrations acquired by two sensors mounted on the both sides of a DaNI robot during a tracing process. Because the relationships imply the effects of flow variation on chemical puffs, a flow sensor is eliminated. To express and maintain the knowledge of chemical concentration changes using the Petri net, we design a mapping algorithm for generating the Petri net from production rules. The Petri net model is implemented on the robot using LabVIEW. The chemical plume tracing experiments achieve 93.8% and 87.5% of source localization rates under both turbulent and diffusive airflow environments, respectively.

1. Introduction

A potential application in expert system research is to develop an intelligent vehicle to search autonomously for sources of hazardous chemicals or pollutants (Bashi-Azghadi, Kerachian, Bazargan-Lari, & Solouki, 2010; Zhou, Huang, & Chan, 2004), victims in earthquake wreckage (Hamp et al., 2014) using expert knowledge of chemical plumes. A critical problem in designing such a system is to construct a navigation mechanism which guides the vehicle to track a chemical plume towards its source. The phenomena of tracking chemical plumes widely exist in a variety of biological behaviors: homing by Pacific salmon (Putman et al., 2013), preying by blue crabs (Kamio, Grimes, Hutchins, Dam, & Derby, 2010; Webster, Volyanskyy, & Weissburg, 2012), and mate-seeking by moths (Allison & Cardé, 2008). Inspired by the behaviors of these animals, researchers started to try building vehicles with similar odor tracing abilities. This research on chemical information-based plume tracing using a vehicle is named as chemical plume tracing (CPT) (Chew, Kishi, Kinowaki, Minegishi, & Kurabayashi, 2013; Farrell, Pang, & Li, 2003; Hayes, Martinoli, & Goodman, 2002; Li, Farrell, & Pang, 2006; Shuo & Farrell, 2006; Webster et al., 2012). In previous work, various biomimetic robotic CPT studies were developed, and advances were achieved in this area. Grasso and Atema (2002) constructed an algorithm in which an autonomous marine robot was navigated using chemical sensing and flow. Farrell, Pang, and Li (2005) presented a CPT approach using a REMUS AUV to trace a chemical plume. This method achieved the average source declaration accuracy of approximately 13 m in a near shore ocean environment. Li et al. (2006) proposed an adaptive mission planner (AMP) strategy, which was inspired by moth behaviors, for finding and tracking a chemical plume and declaring a source location. The strategy was successfully implemented on an AUV and tested in near-shore ocean conditions. The experiments reliably demonstrated the declaration of a source location underwater. Webster et al. (2012) developed a dynamic CPT algorithm inspired by the behaviors of blue crabs in a turbulent flow environment. Success rate and movement patterns compare favorably to that of blue crabs. The above research results, however, are not suitable completely for CPT in airflow environments due to the significant differences between water and an airflow environment in the aspects of kinematics and dynamics (Webster, 2007; Zhang, Cui, & Xu, 2005). A chemical concentration gradient-based approach was presented in Rozas, Morales, and Vega (1991) and Sandini, Lucarini, and Varoli (1993)). A robot

* Corresponding author at: School of Electrical Engineering, Xinjiang University, Urumqi Xinjiang 830047, China. Tel.: +86 151 991 70790.
E-mail addresses: yuanjie222@126.com (J. Yuan), rdoswald@hotmail.com (D. Oswald), wli@csub.edu (W. Li).

http://dx.doi.org/10.1016/j.eswa.2014.08.005
0957-4174/

determined the direction of maximum concentration or higher concentration, and moved toward to it. However, due to the fact that the change of a chemical concentration is relatively slow, there is a low response speed in searching for the direction of maximum chemical concentration, and there is low sensitivity to the changes of chemical concentrations. Thus, it has been a bottleneck issue using chemical concentration gradient in CPT. In the past ten years, few studies solely used this method. Li, Farrell, and Cardé (2001) developed the cross-plume counterturning strategies for maintaining intermittent contact with a chemical plume. The flow direction while detecting odor is the main indicator of the instantaneous desired direction of motion. Lu (2013) investigated indoor odor source localization using a robot equipped with a chemical sensor and a wind sensor. The robot localized the source of an odor plume using chemical concentration and flow information. Moriizumi and Ishida (2002) proposed the transient-response-based algorithm for tracking a chemical plume. The basic strategy in this algorithm is to progress upwind when the robot is in contact with a plume. Flow sensors are necessary components in this system. Russell (2006) developed a search algorithm for tracking chemical plumes in 3-dimensions. An indoor mobile robot was constructed for testing this algorithm. A sensitive azimuth wind vane and an elevation one are mounted in the sensing system of this robot. Harvey, Lu, and Keller (2008) compared four typical insect-inspired chemical plume tracking algorithms using a mobile robot. The four algorithms all use information from a flow sensor and a chemical sensor to guide the agent towards the source of the chemical plume. Although these approaches are effective to track a chemical plume by equipping one or more flow sensors, difficulties may be met under a diffusive environment since the flow information is not reliably acquired.

It has been challenging to develop a generalized algorithm to effectively trace both types of chemical plumes due to the significant differences of their kinetic and dynamic properties. To solve this problem, this study makes the attempt of utilizing the change relationships of chemical concentrations for tracking chemical plumes under both diffusive and turbulent airflow environments. A key issue in this work is how to configure chemical sensors on a mobile robot. Takasaki, Namiki, and Kanzaki (2012) investigated the behavior that male moths located mates, and demonstrated that the difference of the chemical information of left and right antennae affected the walking direction. The bilateral integration of olfactory of biological individuals for odor-source localization can also be found in Duistermars, Chow, and Frye (2009), Gardiner and Atema (2010), Louis, Huber, Benton, Sakmar, and Vosshall (2008), Porter, Craven, and Khan et al. (2007), Rajan, Clement, and Bhalla (2006), and Steck, Knaden, and Hansson (2010). Inspired by the use of bilateral chemical information in the biological behaviors, this study proposes a Petri net (PN)-based CPT approach under both airflow environments. The Petri net is utilized to model the change relationships of chemical concentrations acquired by two sensors mounted on the both sides of a DaNI robot during a tracing process. Because the relationships imply the effects of flow variation on chemical puffs, a flow sensor is eliminated. To the best of our knowledge, there has not been reported in open literature that a generalized algorithm had been developed for tracking effectively chemical plumes under both diffusive and turbulent airflow environments. Therefore, in this work, an exploration of developing a Petri net-based CPT approach for both airflow environments, and favorable experimental results are achieved for both environments.

The rest of this paper is organized as follows. The CPT knowledge is described in Section 2. PN-based CPT approach is presented in Section 3. CPT experiments under both diffusive and turbulent airflow environments are shown in Section 4. Conclusions are drawn in Section 5.

2. CPT knowledge

Chemical concentration information is acquired by two sensors mounted symmetrically in the left and right sides of a DaNI robot. The distance between both chemical sensors should be suitable. The robot fails to move toward a right direction to track a chemical plume when this distance is too small, while the sway amplitude of the robot is large driving toward the chemical source when the distance is too large.

Fig. 1(a)–(l) demonstrate the possible changes under a kind of case that the chemical concentration at the left sensor is higher than that at the right sensor. In each subfigure of Fig. 1, the first solid column and the second column in the left side of a subfigure represent the last and the current sampling values of chemical concentrations acquired by the left sensor, respectively; the columns in the right side denote the values acquired by the right sensor. As shown in Fig. 1(a), the current chemical concentration falls at the left sensor while that at the right sensor remains the same. The control strategy under this case is unchanged according to gradient-based approaches. The other cases in Fig. 1 have similar results. Fig. 1 only shows partial possible change relationships of bilateral chemical concentrations of a mobile robot.

To distinguish among the changes of chemical concentrations, and to has high sensitivities and rapid responses to the changes during a CPT process, this study proposes a PN-based CPT approach under both diffusive and turbulent airflow environments. The approach takes full advantage of the change relationships of the concentrations during a CPT process. The change relationships of chemical concentrations are represented by production rules (PRs), and a Petri net is utilized to model the PRs. According to the Petri net model, a specific control strategy is taken for each change relationship of the bilateral chemical concentrations of a DaNI robot.

2.1. Definitions

For the convenience of describing CPT knowledge, related terms are defined as follows:

Definition 1 (*CL and* ΔCL). Let CL be the output signal voltage of the left chemical sensor, which is proportional to a chemical concentration. The difference between the kth and the $(k-1)$th sampling voltage values of a chemical concentration via left chemical sensor is denoted by $\Delta CL = CL_k - CL_{k-1}$. The absolute value of this difference is represented by $|\Delta CL|$.

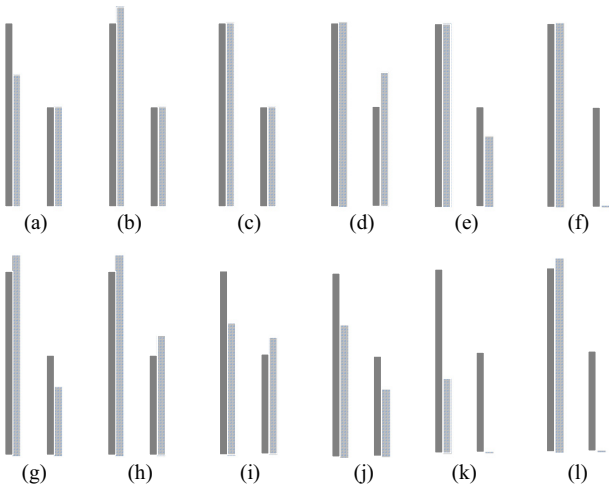

Fig. 1. Possible variances that the chemical concentration at the left sensor is higher than that at the right sensor for two consecutive samples.

Definition 2 (*CR and ΔCR*). Let *CR* be the output signal voltage of the right chemical sensor. The difference between the *k*th and the $(k-1)$th sampling voltage values of a chemical concentration via right chemical sensor is represented by $\Delta CR = CR_k - CR_{k-1}$. The absolute value of this difference is represented by $|\Delta CR|$.

In order to evaluate CPT results under different experimental conditions, the evaluation indices are presented in Definitions 3 to 8.

Definition 3 (*Source localization rate*). A source localization rate is the times of the successful source localization in an experimental group divided by the total number of experiments in the group.

Definition 4 (*Source localization error Δe*). Source localization error Δe is the Euclidean distance between the nominal chemical source location and the source localization position.

Definition 5 (*Accumulate travel distance D_a*). The accumulate travel distance D_a is the total travel distance of a mobile robot from starting a CPT task to end it.

Definition 6 (*Accumulated time t_p*). The time t_p is the accumulated time of tracking a chemical plume during a CPT process.

Definition 7 (*Total time t_a*). The time t_a is the total time during a CPT process.

Definition 8 (*Chemical source localization*). A chemical source is localized when the following conditions are all satisfied. The signal voltage of a chemical sensor is greater than a certain value which may vary from specific experimental conditions; the distance between the robot and an obstacle is less than a threshold, and the total time is less than some value so as to avoid timeout during a CPT process.

2.2. Production rule (PR) based CPT knowledge

The CPT knowledge is represented in a production rule-based form. For the output signal voltages of a chemical sensor, there are four basic variations between two adjacent samples of a chemical, i.e., rise, fall, unchanged, and not available. In the production rule-based knowledge representation, output signal voltage is a linguistic variable, and the four basic variations are the values of the linguistic variable. Moreover, large and small are utilized to depict the properties of linguistic values rise and fall.

Let *R* be a set of production rules: $R = \{R_1, R_2, \ldots, R_m\}$, and a production rule R_i ($i = 1, 2, \ldots, m$) is represented as follows (Bharadwaj & Saroj, 2010; Brachman & Levesque, 2004; Dymova, Sevastianov, & Kaczmarek, 2012; Jaques et al., 2013).

R_i: If *A*, then *B*where $A = \{a_1, a_2, \ldots, a_n\}$represents the antecedent which comprises of one or more propositions connected by "and" in a rule. If one or more propositions are connected by "or" in *A*, then the rule can be transformed into multiple rules in this form R_i.

$B = \{b_1, b_2, \ldots, b_n\}$ represents the consequent which comprises of one or more propositions connected by "and" in a rule.

Partial rules in the CPT knowledge base are listed as follows.

(1) If *CL* rises and $|\Delta CL|$ is large and *CR* rises and $|\Delta CR|$ is large, then robot moves forward.
(2) If *CL* rises and $|\Delta CL|$ is small and *CR* rises and $|\Delta CR|$ is large, then the robot turns right with radius *I*.
(3) If *CL* rises and $|\Delta CL|$ is large and *CR* rises and $|\Delta CR|$ is small, then the robot turns left with radius *II*.
(4) If *CL* rises and $|\Delta CL|$ is small and *CR* rises and $|\Delta CR|$ is small, then the robot moves forward.
(5) If *CL* rises and $|\Delta CL|$ is large and *CR* is unchanged, then the robot turns left with radius *II*.
(6) If *CL* rises and $|\Delta CL|$ is small and *CR* is unchanged, then the robot turns left with radius *I*.
(7) If *CL* rises and $|\Delta CL|$ is large and *CR* falls and $|\Delta CR|$ is large, then the robot turns left with radius *III*.
(8) If *CL* rises and $|\Delta CL|$ is small and *CR* falls and $|\Delta CR|$ is small, then the robot turns left with radius *I*.

In the above rules, *CL* and *CR* are linguistic variables, and rise, fall, unchanged, and not available are linguistic values attached to each linguistic variable. $|\Delta\cdot|$ is small and $|\Delta\cdot|$ is large are the value properties of rise or fall, where $\cdot$ denotes *CL* or *CR*.

3. PN-based CPT approach

Due to the prominent advantages in describing concurrent and asynchronous behaviors, visualizing and maintaining knowledge, Petri nets have been successfully used in the areas of knowledge representation (Liu, Li, & Zhou, 2011;Wang, Peng, Zhu, Hu, & Peng, 2014), modeling (Davidrajuh & Lin, 2011; Lee, 2011; Mayo & Beretta, 2011; Tüysüz & Kahraman, 2010; Vidal, Lama, Diaz-Hermida, & Bugarin, 2013), monitoring (Liu et al., 2011), predicting (Yu & Frincke, 2007), and diagnosis (Bouali, Barger, & Schon, 2012; Mansour, Wahab, & Soliman, 2013; Renganathan & Bhaskar, 2013; Yang, Jeong, Oh, & Tan, 2004). In this work, the change relationships of chemical concentrations during a tracing process are represented by production rules (PRs); a Petri net is utilized to model the PRs for the following reasons. (1) Efficient knowledge updates. In a knowledge base, if a rule component shared by multiple different rules needs to be modified, only the place corresponding to the component is modified in the PNs. By contrast, the rules sharing the component need to be totally modified in the whole knowledge base. It is especially a time-consuming and difficult task for a large and complex knowledge base. (2) Behavior analysis. When one or multiple object places, which represent the robot behaviors, are selected, sub-PNs including the object places can be abstracted automatically via the computation of incidence matrices of the PNs, and the unrelated nodes are filtered, simplifying the complexity of behavior analysis. (3) Structured programming, especially for graphical programming languages, such as LabVIEW. Programming efficiency is improved, and readability and reusing of codes can be enhanced using the PN model.

3.1. PN-based CPT system model

A PN based CPT system model is shown in Fig. 2. In this model, a CPT knowledge base consists of CPT rules, system parameters and basic data, which are acquired via a knowledge acquisition module. CPT rules are mapped into PNs according to a model mapping algorithm. Concentration information is sampled via chemical sensors, and the information is then processed in a module. The processed data is input into a model match module to match with PN models. System parameters and CPT basic data in the knowledge base provide supporting data to the match module. The matching results generate a control strategy for a mobile robot to perform a CPT behavior. Control parameters are input to the actuators of the robot; the outputs of the actuators are gauged via a measure device, and are fed back to a comparator to form a closed loop control. In this work, the focus is on the PN-based CPT models and algorithm under both diffusive and turbulent airflow environments.

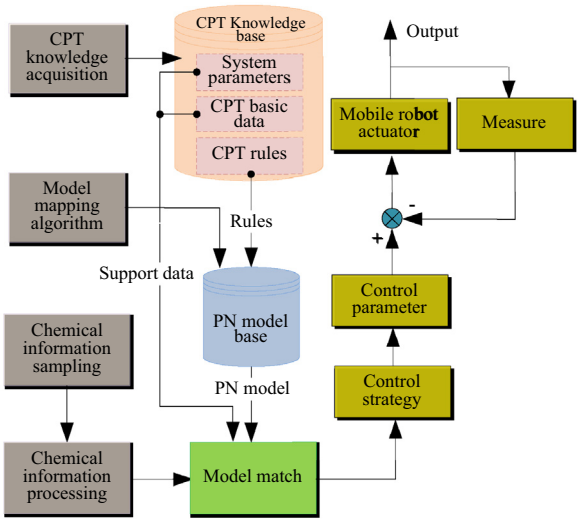

Fig. 2. PN-based CPT system model.

3.2. Petri nets (PNs)

In this part, we present basic concepts about Petri nets (Formanowicz, Kozak, Glowacki, Radom, & Formanowicz, 2013; Jiang, 2004; Lee, 2011; Mansour et al., 2013; Yuan, 2005). A Petri net is defined as a 3-tuple:

$PN = (P, T, F)$

where

$P = \{p_1, p_2, \ldots, p_n\}$ is a finite set of places.
$T = \{t_1, t_2, \ldots, t_m\}$ is a finite set of transitions, and $P \cap T = \varnothing$.
$F \subseteq (P \times T) \cup (T \times P)$ is a set of directional weighted arcs connected places and transitions, where $\times$ denotes a Cartesian product.

Graphically, a place is denoted by a circle, a transition is denoted by a rectangle, and a directional arc is represented by a directional arrow connecting a place and a transition.

Definition 9 (*Marking*). m: $P \to N$ is called a marking, where $N = \{0, 1, 2, \ldots\}$. m is a column vector, and the ith element of the vector denotes the number of tokens in the ith place.

Definition 10 (*Pre-set*). $\forall x \in P \cup T$, $\cdot x = \{y | (y, x) \in F\}$ is called the pre-set of x.

Definition 11 (*Post-set*). $\forall x \in P \cup T$, $x\cdot = \{z | (x, z) \in F\}$ is called the post-set of x.

Definition 12 (*Input place*). $\forall p \in P$, $\forall t \in T$, if $p \in \cdot t$, then place p is called the input place of transition t.

Definition 13 (*Output place*). $\forall p \in P$, $\forall t \in T$, if $p \in t\cdot$, then place p is called the output place of transition t.

Definition 14 (*Firing conditions*). A transition $t \in T$ can be fired under marking m if and only if: $\forall p \in \cdot t : m(p) \geqslant I(p, t)$, where $\cdot t$ denotes a pre-set of transition t, $m(p)$ denotes the number of tokens in place p under marking m, and $I(p, t)$ represents the weight of the directional arc from place p to transition t.

Definition 15 (*Firing process*). Once a transition t satisfies the firing conditions, then t is enabled. After t is fired, $\forall p \in t\cdot$, $m(p) = 1$.

In this study, a place represents a piece of information rather than a resource, and the information is either true or false, thus $|token| \in \{0, 1\}$, where $|\cdot|$ represents the number of tokens. A token is equal to one. The weights of the arcs are all ones.

3.3. Mapping model and algorithms for CPT

3.3.1. Mapping model

The mapping model between production rules and Petri nets is shown in Fig. 3.

In Fig. 3, "◇" denotes "consists of", and "..*" denotes "or multiple". The light rectangles containing words are the elements of rules. The elements of a Petri net include a solid thin rectangle at the bottom of this figure, the three solid circles, and the solid arrows connected them. The dash arrows represent the mapping operations between a rule element and a PN element.

3.3.2. Mapping algorithm

For generating automatically Petri nets from a PR set, in this part, we propose a mapping algorithm. This algorithm is presented in a pseudo code form.

Let P, T, F, V, S, C be null sets, where V is a linguistic value set, S is a value property set, and C is a set of the consequents of rules. Let $v_k^l (k = 1, 2, \ldots)$ be a variable value of linguistic variable l in a proposition. Let s_j $(j = 1, 2, \ldots)$ be a value property of the linguistic value v_k^l in the proposition.

Algorithm: Generating Petri nets from a PR set

Input: Production rule set (R)
Output: Petri net (P, T, F)
  while R is not a null set, **do**
  Take out a rule r_i from set R
  $R = R - \{r_i\}$
  A transition t_i is assigned to r_i
  $T = \{t_i\} \cup T$
  for all parts of rule r_i, **do**
    if the part is an antecedent, **then**
      for all propositions in this part, **do**
        if there is not a value property in v_k^l, **then**
          if $v_k^l \notin V$, **then**
          $V = \{v_k^l\} \cup V$, $v_k^l \to p_k$
          $P = \{p_k\} \cup P$, and $F = \{f_{ki}\} \cup F$
        end if
      end if
      if $s_j \notin S$, **then**
        $S = \{s_j\} \cup S$, $s_j \to p_j$
        $P = \{p_j\} \cup P$, $F = \{f_{ji}\} \cup F$
      end if
    end for
  end if
  if this part is a consequent c_q, **then**
    if $c_q \notin C$, **then**
      $c_q \to p_q$, $P = P \cup \{p_q\}$
      $F = \{f_{iq}\} \cup F$
      end if
    end if
  end for
end while

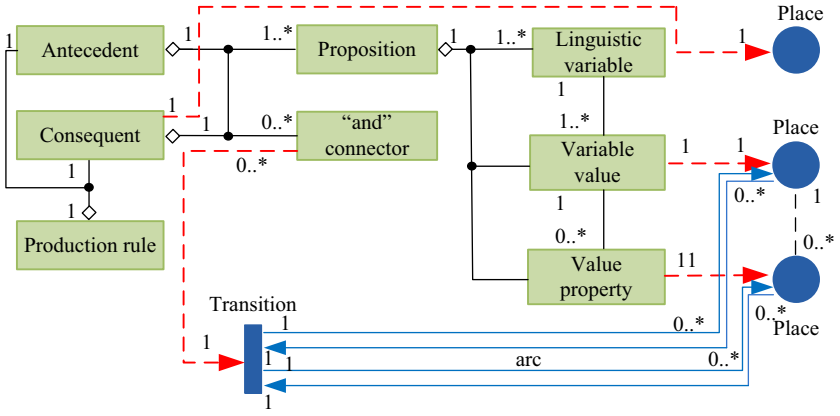

Fig. 3. CPT mapping model between production rules and Petri nets.

In the above algorithm, "→" denotes a transformation operation; f_{ki} is a directional arc from place p_k to transition t_i, where $i = 1, 2, \ldots$; f_{ji} is a directional arc from place p_j to transition t_i; f_{iq} is a directional arc from transition t_i to place p_q, where $q = 1, 2, \ldots$

3.4. PN-based CPT model

By the above mapping algorithm, a Petri net model is constructed on the basis of the CPT knowledge presented in Section 2.2. The partial Petri net model is shown in Fig. 4.

The PN model consists of three layers, i.e., a knowledge description layer, a knowledge correlation layer, and a control strategy layer. The layers are separated by two vertical dot-dash lines. In knowledge description layer, a dash line connects a place and a linguistic variable.

In Fig. 4, the places in the first column are mapped by linguistic values in the antecedents of rules; the places in the second column are mapped by value properties, and the places in the last column are mapped by the consequents of rules. A rectangle represents a transition. The meanings of the places are given in Table 1.

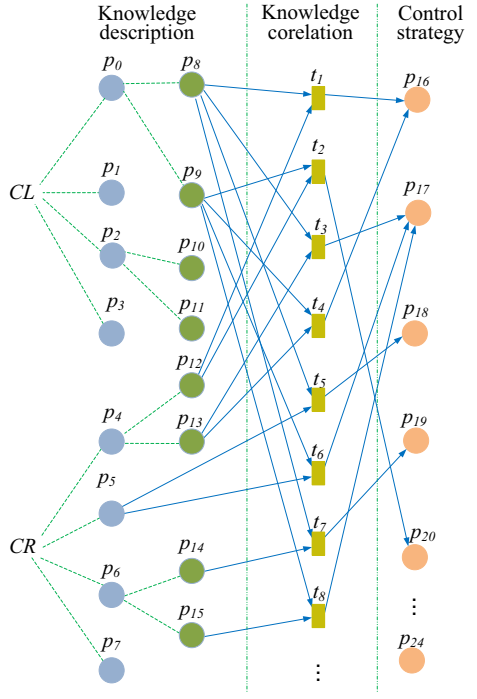

Fig. 4. Partial Petri net model for a chemical plume tracing process.

In Table 1, linguistic value "rise" is defined as $\Delta\cdot > 0.005$, "unchanged" is defined as $|\Delta\cdot| \leqslant 0.005$, and "fall" is $\Delta\cdot < -0.005$, where "·" denotes *CL* or *CR*, and "Δ" is interpreted in Definition 1 and Definition 2. "$|\Delta\cdot|$ is large when · rises" is defined as $|\Delta\cdot| > 0.01$; "$|\Delta\cdot|$ is small when · rises" is $0.005 < \Delta\cdot \leqslant 0.01$; "$|\Delta\cdot|$ is large when · falls" is $\Delta\cdot < -0.01$; "$|\Delta\cdot|$ is small when · falls" is $-0.01 \leqslant \Delta\cdot < -0.005$. "Run forward" is defined as angular velocities of both motors are 0.8 rad/s; "radius *I*" is angular velocities of both motors are 0.8 and1.6 rad/s, respectively; "radius *II*" is angular velocities of both motors are 0.8 and 2.0 rad/s, respectively; "radius *III*" is angular velocities of both motors are 0.8 and 2.4 rad/s, respectively; "wait" represents angular velocities of both motors are 0 rad/s.

3.5. PN-based CPT programming procedures

The Petri net is implemented using LabVIEW, and the programming procedures are listed as follows.

Table 1
Meanings of places.

Place	Meanings
p_0	*CL* rises
p_1	*CL* is unchanged
p_2	*CL* falls
p_3	*CL* is not available, i.e., $CL_k \leqslant CL_n$
p_4	*CR* rises
p_5	*CR* is unchanged
p_6	*CR* falls
p_7	*CR* is not available, i.e., $CR_k \leqslant CR_n$
p_8	$\|\Delta CL\|$ is large when *CL* rises
p_9	$\|\Delta CL\|$ is small when *CL* rises
p_{10}	$\|\Delta CL\|$ is large when *CL* falls
p_{11}	$\|\Delta CL\|$ is small when *CL* falls
p_{12}	$\|\Delta CR\|$ is large when *CR* rises
p_{13}	*CR* rises and $\|\Delta CR\|$ is small
p_{14}	*CR* falls and $\|\Delta CR\|$ is large
p_{15}	*CR* falls and $\|\Delta CR\|$ is small
p_{16}	Run forward
p_{17}	Turn left with radius I
p_{18}	Turn left with radius II
p_{19}	Turn left with radius III
p_{20}	Turn right with radius I
p_{21}	Turn right with radius II
p_{22}	Turn right with radius III
p_{23}	Wait
p_{24}	Reacquire a chemical plume

Step 1: Set sampling channels for both chemical sensors. The channel addresses correspond to the physical addresses of the signal sampling module of the DaNI robot. Because output signal voltages of a chemical sensor are analog data, analog input channels are selected in a software configuration module.

Step 2: Set sampling frequency f. f must satisfy the Shannon's sampling theorem, (Tan, 2007) i.e., $f > 2f_{smax}$, where f_{smax} denotes the highest frequency of a signal.

Step 3: Design the filters of input chemical signals. In order to resist interference, moving average filters (Wang, 2003) are utilized to smooth the chemical signal voltages. The parameter n in a filter should be suitable for the signal. If n is set to be too large, the sensitivity of the signal is low. By contrast, if n is set to be too small, the smoothness of the signal is weak.

Step 4: Set the benchmark voltages for two input channels of the chemical sensors without chemical. The benchmark voltages of chemical signals are set ahead of performing CPT. Let C_n be an output signal voltage of a chemical sensor under no chemical in an airflow environment. When the output signal voltage of a sensor is greater than C_n, a chemical is detected.

Step 5: Define the places according to the knowledge description layer in the PN model. A place in the knowledge description layer is an input place of a transition. A place in the layer is represented as one or more expressions.

Step 6: Define the places in the control strategy layer of the PN model. A place in control strategy layer is an output place of a transition. The place corresponds to a control strategy in a control module, and can be represented by a condition in a case structure. The control strategy provides a pair of control values to the drive motors of the robot.

Step 7: Define the transitions and arcs according to the knowledge correlation layer in the PN model. An arc connects a place and a transition. A transition connects two input places and an output place in the model. If and only if tokens exist in the two input places, the transition can be fired. An action and two conditions correspond to the output place and the two input places of the transition, respectively. The action can be carried out when the two conditions are satisfied.

Step 8: Set stop conditions. The CPT program will be ended when either of the following conditions are met. (1) The distance between a supersonic sensor and an obstacle is less than a certain value. (2) The total time of CPT is larger than some value.

4. Experiments

The goal of the experiments is to analyze the performance of the proposed PN-based CPT approach.

4.1. Experimental platform

A DaNI robot platform for tracking a chemical plume is shown in Fig. 5.

An ultrasonic transducer PING28015 at the front center position of the DaNI robot is utilized to detect an obstacle. The transducer has a detection range of 0.02–3 m. Two DC drive gear motors of Pitsco 39083 are used to drive the robot wheels. The motors run at 146 to 152 rpm under no load. The speed of the motors is adjusted with a pulse width modulation (PWM) technique. Two NI encoder kits of W35915 with a resolution of 100CPR are fitted in two differential wheel shafts, respectively. Position and direction feedback from the encoders are read as inputs by a control module, and are implemented in programming for tracking the rotational data of the drive motor shafts. The encoders allow the robot to move a fixed distance, rotate a specific amount, and move at a certain speed. Chemical is pumped by a humidifier of Crane EE 5301 W. Two chemical sensor circuit boards are mounted symmetrically in both sides of the DaNI robot. The type of the chemical sensors in the circuit boards is TGS2620. The chemical sensors have high sensitivity to the vapors of organic solvents, volatile vapors, and combustible gases such as carbon monoxide. The plane on which the two chemical sensors stand is parallel with the shaft line of both drive wheels. The output signal voltage of a chemical sensor circuit board is proportional to the concentration of a chemical. The concentration detection range of a chemical sensor circuit is 50–5000 ppm. The chemical signal output voltage range in a chemical sensor circuit is 0.5–3.8 V, and the detected signal resolution is 0.0001 V. A program is downloaded from a computer to the robot via a wireless LAN. A wireless adapter of EDIMAX USB EW7811UTn with 150 Mbps is connected to the computer, and a wireless router TL-WR841N is connected to the robot. The programming environment is LabVIEW2012 and a Robotics module. A LabVIEW program consists of front panels and block diagrams. They are executed by the robot and the computer synchronously. The real-time communication between them is implemented via the wireless LAN.

4.2. PN model-based programs

Two analog sampling channels AI_0 and AI_1 are set for both chemical sensor circuits, respectively. Two moving average filters are used, and the parameter n is set to be 5 for achieving a good balance between high sensitivity and a smoothness of the signals. Let CL_n and CR_n be the output signal voltages of both chemical sensor circuits under no chemical, respectively. The CPT program will be stopped when the distance between the ultrasonic sensor and an obstacle is less than 0.2 m, or when the total time of CPT is larger than or equal to 150 s.

Fig. 6 shows partial LabVIEW programs of the CPT algorithm. Fig. 6(a) partially presents the place definitions in the knowledge description layer of the PN model. The index of an element in an array denotes a place in this layer, while the element in the array corresponds to a token. Fig. 6(b) demonstrates the relationships between transitions and places. An operator "^" represents a transition. Fig. 6(c) presents the place definitions in the control strategy layer of the PN model. A condition of the case structure corresponds to a place in this layer. Fig. 6(d) shows the program of a filter. The filter is utilized to smooth the chemical signal voltages.

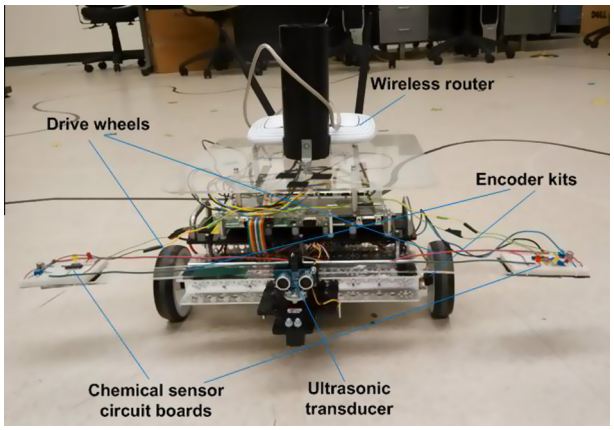

Fig. 5. DaNI robot platform for tracking a chemical plume.

4.3. Environmental conditions and parameters

A 3.8 m by 4.6 m arena area in a lab is utilized to test the PN-based CPT approach. The origin of location coordinates is located at the lower left corner of the experimental area. The chemical source location is at (1.56, 3.61) m. The starting position of the robot is (0.8, 0.7) m, and the directional angles is −5°. The initial distance between the robot and the chemical source is 3 m. Through CPT experimental tests on the variable distances between both chemical sensors, the distance is set to be 0.65 m for obtaining a right tracking direction and small sway amplitude of the robot. The spout height of the humidifier is 0.34 m. The experiments are split into six groups whose IDs range from Group *I* to *VI*. Each group consists of 16 CPT experiments under same experimental conditions. The conditions and experimental parameters are summarized in Table 2. The turbulence airflow was generated by an electrical fan. This fan changed the speeds and directions of the chemical plumes dynamically via swinging its head. Both parameters of the chemical plumes were measured by a Gill WindSonic wind sensor. The wind sensor is connected to another DaNI robot via a RS232 serial port. The VISA Configure Serial Port VI of LabVIEW is used and is initialized by "VISA resource name" to the specified settings. This serial port works at a baud rate of 9600 b/s. This VI writes data from a write buffer to the interface specified by "VISA resource name". The VI reads the data form the interface and returns the data in a "read buffer". When the chemical is identified, the wind sensor records the real-time speeds and directions of the current plume. Note that the parameters of a chemical plume are not used for tracking chemical plumes, they only indicate the current CPT environments. Sampling period is set up in a while-loop structure using a "Wait Until Next ms Multiple" millisecond timer function in the block diagram of the CPT LabVIEW program. Chemical release rate is measured by weighing the humidifier using a precision electric balance with 0.01 grams readability. The chemical source localization criterion satisfies all the conditions: the distance between the DaNI robot and an obstacle is less than 0.35 m; the total CPT time is less than 150 s; the signal voltage of a chemical sensor is greater than the corresponding threshold voltage presented in Table 2.

4.4. Results and analysis

4.4.1. CPT results under a diffusive and a turbulent airflow environment

A practical CPT process under a diffusive airflow environment is shown in Fig. 7(a)–(d). The experimental parameters of this process are presented in Group *I* of Table 2. In Fig. 7, a time unit represents 0.4 s in the figures. Fig. 7(a) shows the signal voltages of both chemical sensors before filtering. The thin curve denotes the voltages of the left chemical sensor, and the thick curve displays the voltages of the right sensor. The signal voltages of the chemical sensor circuit boards indicate the magnitudes of the concentrations of a chemical.

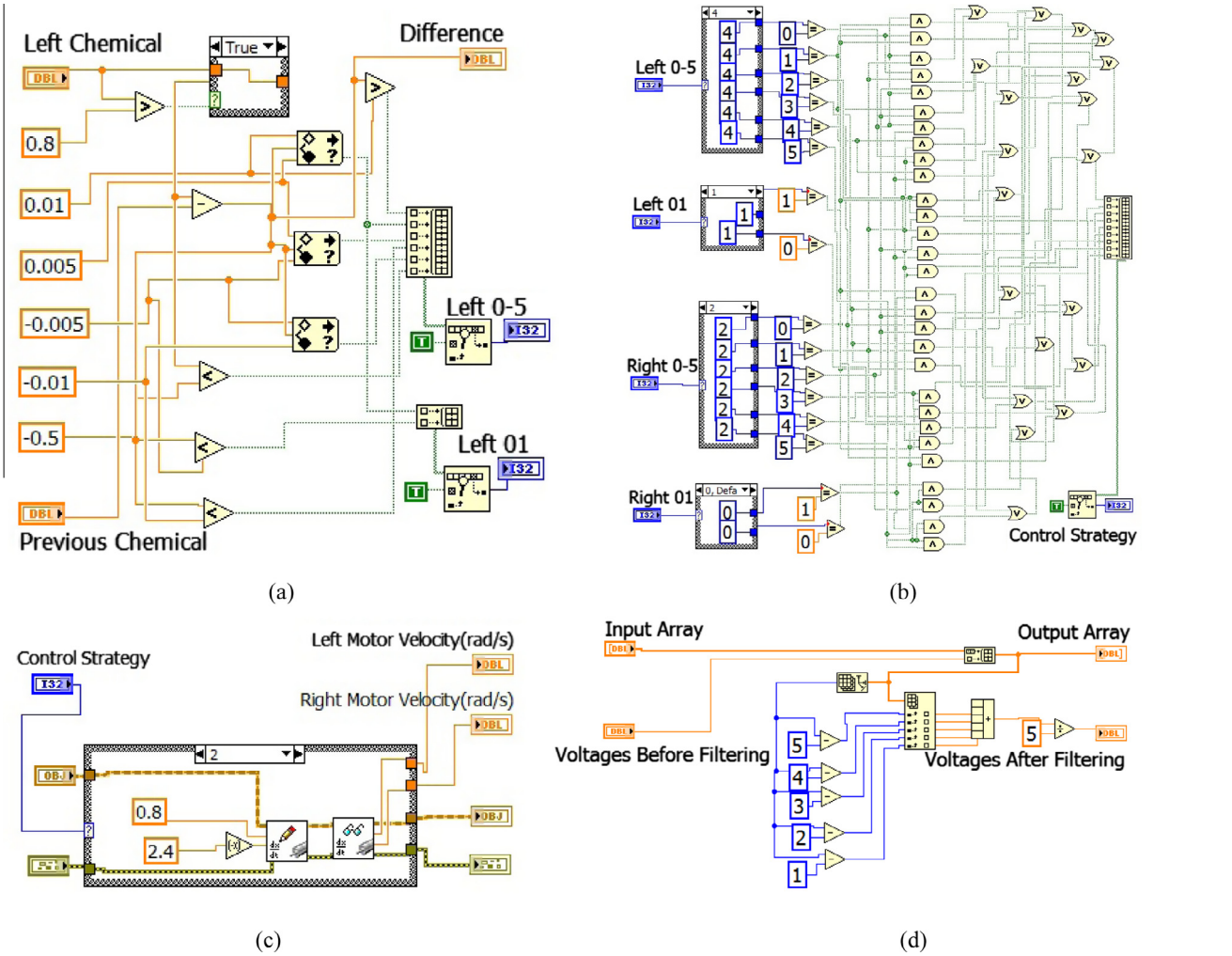

Fig. 6. Partial CPT programs based on PN model.

Table 2
CPT conditions and parameters.

Group ID	Range of plume speed and direction	Height of chemical sensors, meters	Sampling period, seconds	Chemical release rate, gram/min	Benchmark voltages of chemical sensors without chemical, volts		Threshold voltages of chemical sensors for source localization, volts	
					Left side	Right side	Left side	Right side
I	N/A	0.108	0.2	1	1.05	1.22	2.48	2.65
II	[0.04, 0.06] (m/s) [60–120°]	0.108	0.2	1.4	1.08	1.25	1.98	2.15
III	N/A	0.108	0.4	1	1.04	1.21	2.28	2.45
IV	[0.04, 0.06] (m/s) [60–120°]	0.108	0.4	1.4	1.06	1.24	1.73	1.9
V	N/A	0.221	0.2	1	0.88	1.05	1.66	1.83
VI	[0.04, 0.06] (m/s) [60–120°]	0.221	0.2	1.4	0.85	1.02	1.54	1.71

The bigger the signal voltage is, the higher the concentration of the chemical is. Fig. 7(b) shows the signal voltages of both chemical sensors after filtering. Fig. 7(c) displays the voltage differences between the current and the previous samples of the chemical sensors after filtering. The thin curve and the thick one present the differences of left and right sensors, respectively. According to the Table 1, a voltage difference corresponds to a token of a place in the knowledge described layer of the PN model. Fig. 7(d) displays the travel distances of both drive wheels of the robot. The thin curve and the thick one show the travel distances of the left and right drive wheels, respectively. During the period of a sample time interval, the distances traveled by both wheels of the robot indicate the current control strategy. For instance, the robot runs forward when the distances traveled by both wheels are equal.

The CPT process under the diffusive airflow environment can be separated into three stages. In the period of time between 10 and 70 units shown in Fig. 7(b), the output signal voltages of the left sensor ranges from 1.69 to 1.82 V, and that of the right sensor ranges from 1.83 to 1.91 V. The average rate of change of the left chemical sensor is 0.0022 V for each time unit, and that for the right sensor is 0.0013 V. The signal voltages of both chemical sensors are at lower values and have subtle changes at this stage. It indicates that the distance between the robot and the chemical source is far during this period. In the period of time between 70 and 93 units, the signal voltages of the left chemical sensor rises from 1.81 to 2.38 V, and for the right sensor rises from 1.91 to 2.37 V. The average rates of change of the left and right chemical sensors are 0.0248 and 0.02 V for each time unit, respectively. They

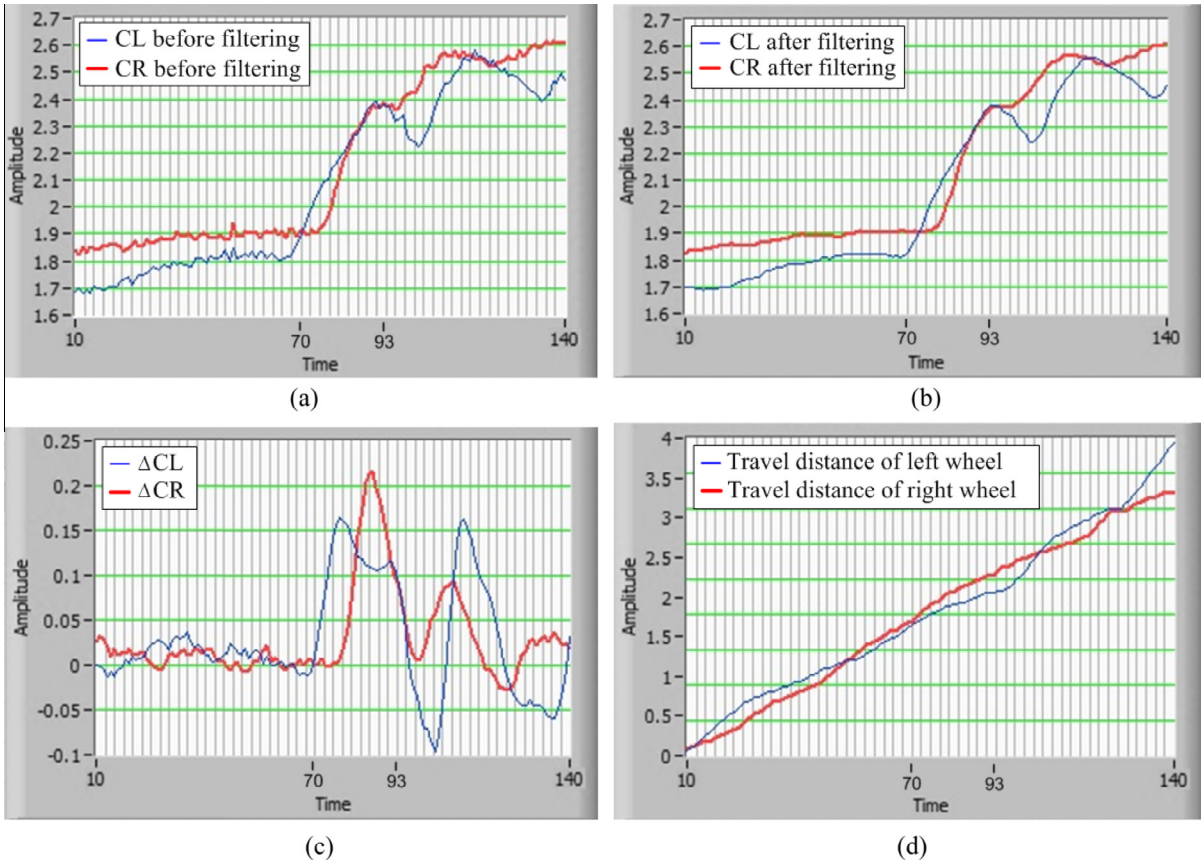

Fig. 7. Practical CPT process under a diffusive airflow environment.

are almost ten times that of the last stage. The signal voltages of both sensors are at medium values and have evident changes at this period. It implies that the robot is approaching the vicinity of the chemical source for this duration. In the period of time between 93 and 140 units, the signal voltages of the left chemical sensor range from 2.23 to 2.59 V with the rate of change 0.0077 V for each time unit. The voltages of the right sensor rise from 2.37 to 2.61 V with the rate of change 0.0051 V. It suggests that the robot is approaching the center of the chemical source at this stage. In this CPT process under the diffusive airflow environment, source localization error Δe is 0.212 m; accumulate travel distance D_a is 3.62 m; the accumulated tracking time t_p is 51.8 s; the total time t_a is 55.9 s.

For analyzing the CPT process implemented by the Petri net model, the partial amplified graphs of Fig. 7(c) and (d) is presented in Fig. 8(a) and (b), respectively. A time grid in Fig. 8(a) and (b) represents a time unit, and that is 0.4 s. The control decision processes of the robot depend on the Petri net model shown in Fig. 4. For example, at 117 units of the time axis in Fig. 8(a), the difference between two adjacent sampling signal voltages of the left sensor is 0.089 V, which is greater than 0.01 V. It indicates that there exists a token in place p_8 of the PN model. At the same position of the time axis, the difference for the right sensor is −0.004 V, and is greater than −0.005 V. It indicates that there exists a token in place p_5. According to the PN model shown in Fig. 4 as well as Definition 14 and 15, transition t_5 is fired, and place p_{18} acquires a token. Therefore, the current control strategy is that the robot turns left with radius *II*. According to the place definition of p_{18} presented in Table 2, the angular velocities of the left and right motors of the robot are 0.8 and 2.0 rad/s, respectively. It can be inferred that the right wheel will run further distance than the left wheel for the next running period. In the period of time between 117 and 122 units of the time axis of Fig. 8(b), the left wheel traveled 0.12 m, while the right wheel traveled 0.32 m, and the robot turned left. Therefore, the two corresponding values of both curves at any point of the time axis in Fig. 8(a) correspond to two tokens of places in the knowledge described layer of the PN model; some transition can be fired at the current status; a place in control strategy layer acquires a token, which indicates that a certain control strategy is performed.

A practical CPT process under a turbulent airflow environment is presented in Fig. 9(a)–(d). The experimental parameters of this process are presented in Group *II* of Table 2. In Fig. 9, a time unit represents 0.4 s in the figures. The meanings of the curves in Fig. 9(a)–(d) are the same as those of Fig. 7(a)–(d), respectively. Compared with Fig. 7(b), the first stage in Fig. 9(b) is the period of time between 11 and 36 units, which is 48.6% shorter than that of Fig. 7(b). Unlike that of the last case in a diffusive airflow environment, there is not an evident boundary between the second stage and the third one during the CPT process in Fig. 9(b). The two stages span the period of time between 36 and 141 units, and cover the 74.5% of the CPT process. The maximum value of the differences between both adjacent samples of the chemical sensors is 0.088, while the value in Fig. 7(c) is 0.22 which appears in its second stage. It implies that the chemical plume has a better diffusion effect in a turbulent airflow environment. In the same principle as the last case, two values of both curves at any point of time axis in Fig. 9(c) generate some control strategy to be executed for the next running period according to the PN model, and the corresponding travel distances of both drive wheels are presented in Fig. 9(d). In this CPT process under the turbulent airflow environment, source localization error Δe is 0.226 m; accumulate travel distance D_a is 3.48 m; the accumulated tracking time t_p is 52.4 s; the total time t_a is 56.5 s.

4.4.2. CPT grouping results

The CPT results of the groups in Table 2 are presented in Table 3. Group *I* is the experiments in a diffusive airflow environment with the sampling period of 0.2 s, while Group *II* is in a turbulent airflow environment with the same sampling period. The average source localization error of Group *II* is 0.035 m greater than that of Group *I*. The other index values of Group *II* is better than Group *I*. This is because that the proposed PN-based CPT approach in a turbulent environment has a quicker response than that in a diffusive airflow environment. In Groups *III* and *IV*, the sampling periods increase to 0.4 s, and the corresponding CPT results can be interpreted by the similar reasons to those of Groups *I* and *II*. In Groups *V* and *VI*, the heights of the chemical sensors increase to 0.221 m, and the CPT effects become worse than those of Groups *I* and *II*. The reason is that the average relative molecular weight of the chemical is larger than the air, and detecting the chemical become more difficult at the current height of the chemical sensors than in Group *I* to *II*. In Groups *I* and *III*, the sampling periods are 0.2 and 0.4 s respectively, and the experiments are performed under diffusive airflow environments. The CPT effects in Group *I* are better than Group *III*. In Groups *II* and *IV*, the sampling periods are 0.2 and 0.4 s respectively, and the experiments are tested under turbulent airflow environments. A similar conclusion can be drawn as that of Groups *I* and *III*. It suggests that the sampling periods should not be set too large, which may result in slow response to the changes of a chemical. As a result, the proposed PN-based CPT approach can achieve favorable CPT effects under both turbulent and diffusive environments.

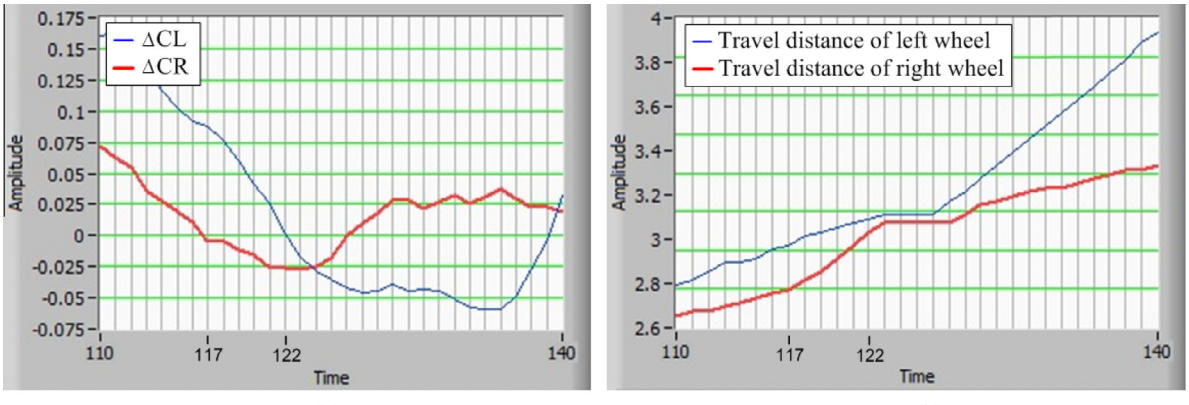

(a) (b)

Fig. 8. Partial amplified graphs for output signal voltages and accumulated travel distances.

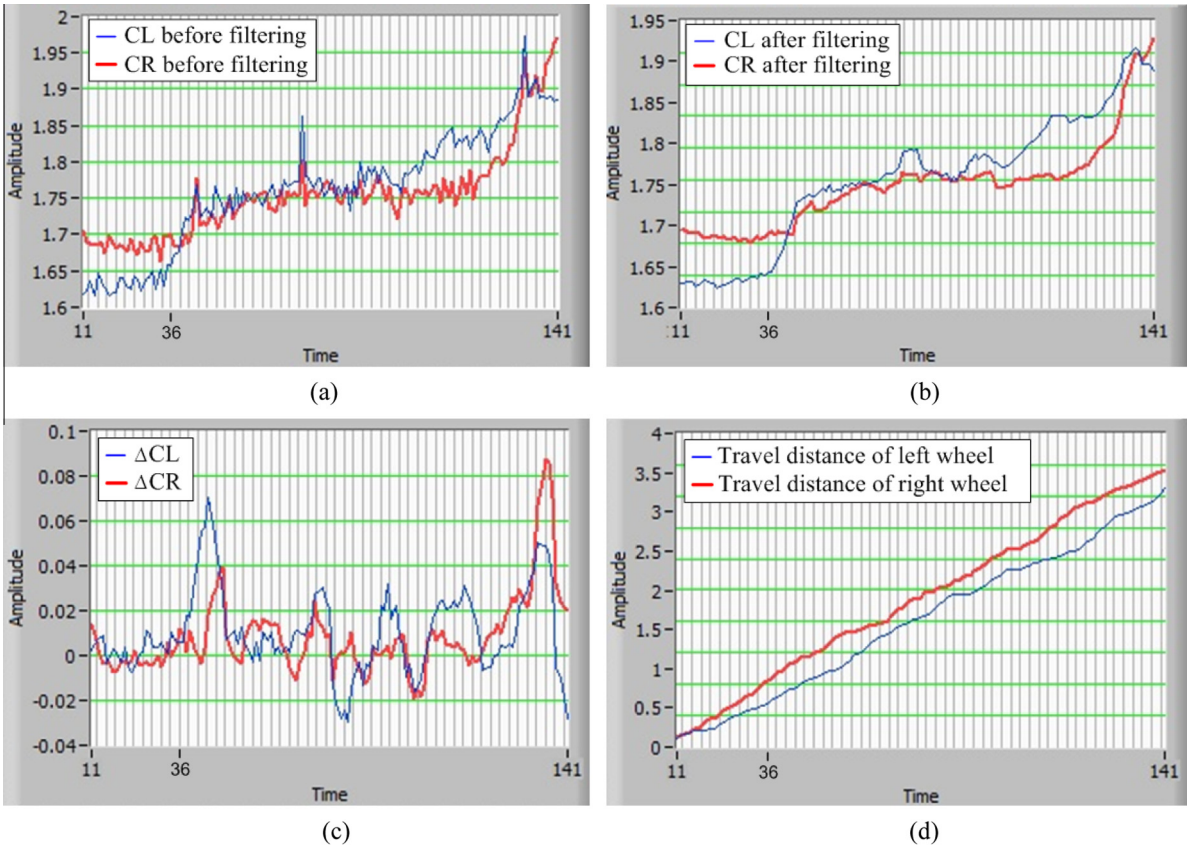

Fig. 9. Practical CPT process under a turbulent airflow environment.

Table 3
CPT grouping results.

Group ID	Source localization rate, percentage	Average source localization error, meters; σ_e	Average accumulate travel distance D_a, meters; σ_d	Average time to trace plume t_p, seconds; σ_{tp}	Average total time t_a, seconds; σ_{ta}
I	**87.5%**	**0.197**	**3.63**	**63.6**	**69.8**
		0.089	**0.19**	**2.3**	**2.5**
II	**93.8%**	**0.232**	**3.45**	**52.8**	**59.2**
		0.040	**0.11**	**1.7**	**1.9**
III	75.0%	0.283	3.92	71.1	89.5
		0.065	0.19	3.4	3.9
IV	81.2%	0.298	3.73	74.9	83.1
		0.043	0.16	3.2	3.6
V	62.5%	0.373	4.13	76.2	106.7
		0.099	0.47	8.6	10.9
VI	68.8%	0.382	3.96	89.7	101.2
		0.124	0.36	8.0	8.3

The bold values display the best results of the CPT experiments under diffusive and turbulent airflow environments, respectively.

5. Conclusions

It has been challenging to develop a generalized algorithm to effectively trace the chemical plumes in both diffusive and turbulent airflow environments. This study presents a Petri net based chemical plume tracing approach under both airflow environments. Inspired by the use of bilateral chemical information in the biological behaviors, two chemical sensors are mounted symmetrically on both sides of a DaNI robot to acquire the chemical concentrations during a tracing process. The change relationships of chemical concentrations during a tracing process are represented by production rules (PRs). Due to the prominent advantages in maintaining knowledge, analyzing behaviors, and visualizing knowledge, a Petri net is utilized to model the PRs. Because the relationships imply the effects of flow variation on chemical puffs, a flow sensor is eliminated in this work. This is the major progress for achieving a CPT process without a flow sensor under a turbulent airflow environment.

The CPT experiments achieve 93.8% and 87.5% of source localization rates under turbulent and diffusive airflow environments, respectively. Under the turbulent airflow environments, the average accumulate travel distance and the average total time are 3.45 m and 59.2 s, respectively. Under the diffusive airflow environments, the average accumulate travel distance and the average total time are 3.63 m and 69.8 s, respectively.

In this study, a PN-based CPT system model is presented, a mapping model between production rules and Petri nets is given. For generating Petri nets from a PR set automatically, we propose a

mapping algorithm. A Petri net model is utilized to model the expert knowledge of chemical plumes. The PN model is constructed according to this mapping algorithm. The PN model is clearly separated into three layers: a knowledge description layer, a knowledge correlation layer, and a control strategy layer. According to the PN model, a specific control strategy is taken for each single change relationship of the bilateral chemical concentrations of a DaNI robot. The programming procedures are given, and the PN model is programmed using LabVIEW on a DaNI robot platform. The aforementioned models and algorithms also provide references for the design and development of other expert systems.

During a CPT process, partial parameter settings can affect the CPT performances. The distance between both chemical sensors of the robot, for instance, should be suitable. The robot fails to move toward a right direction to track a chemical plume when this distance is too small, while the sway amplitude of the robot is large driving toward the chemical source when the distance is too large. The distance between both chemical sensor boards is 0.65 m in this work. The heights of the chemical sensors can also affect the CPT results. The CPT source location rate at the sensor height of 0.108 m is higher than that of 0.221 m. The reason is that the average relative molecular weight of the chemical is larger than the air, and detecting the chemical become easier at the sensor height of 0.108 m than that of 0.221 m. The sampling periods should not be set too large, because this may result in slow response to the changes of a chemical. In this work, the possible reasons for unsuccessful CPT experiments include: There still exists room for optimizing partial experimental parameters, and there still exists room for improving CPT knowledge.

Several future research directions include: (a) Self-optimizing approach for knowledge acquisition. (b) Rule learning for complex and large knowledge systems using fuzzy Petri nets. (c) Information fusion for a knowledge-based system. (d) Parameter sensitivity analysis for a multi-sensor system.

Acknowledgments

The authors gratefully acknowledge financial support from National Natural Science Foundation of China under Grant 61164012 and China Scholarship Council under Grant 20125030. This research is conducted in Robotics Lab, California State University, Bakersfield.

References

Allison, J. D., & Cardé, R. T. (2008). Male pheromone blend preference function measured in choice and no-choice wind tunnel trials with almond moths, Cadra cautella. *Animal Behaviour, 75*(1), 259–266.

Bashi-Azghadi, S. N., Kerachian, R., Bazargan-Lari, M. R., & Solouki, K. (2010). Characterizing an unknown pollution source in groundwater resources systems using PSVM and PNN. *Expert Systems with Applications, 37*(10), 7154–7161.

Bharadwaj, K. K., & Saroj (2010). A parallel genetic programming based intelligent miner for discovery of censored production rules with fuzzy hierarchy. *Expert Systems with Applications, 37*(6), 4601–4610.

Bouali, M., Barger, P., & Schon, W. (2012). Backward reachability of colored Petri nets for systems diagnosis. *Reliability Engineering & System Safety, 99*(3), 1–14.

Brachman, R. J., & Levesque, H. J. (2004). *Knowledge representation and reasoning*. San Francisco, CA: Morgan Kaufmann Publishers (pp. 118–130).

Chew, J. Y., Kishi, K., Kinowaki, Y., Minegishi, R. & Kurabayashi, D. (2013). A Tethered system to investigate the behavioral changes of the silk moth for chemical plume tracing. In *Proceedings of 2013 10th international conference on ubiquitous robots and ambient intelligence (URAI)* (pp. 37–38).

Davidrajuh, R., & Lin, B. (2011). Exploring airport traffic capability using Petri net based model. *Expert Systems with Applications, 38*(9), 10923–10931.

Duistermars, B. J., Chow, D. M., & Frye, M. A. (2009). Flies require bilateral sensory input to track odor gradients in flight. *Current Biology, 19*(15), 1301–1307.

Dymova, L., Sevastianov, P., & Kaczmarek, K. (2012). A stock trading expert system based on the rule-base evidential reasoning using level 2 quotes. *Expert Systems with Applications, 39*(8), 7150–7157.

Farrell, J. A., Pang, S., & Li, W. (2003). Plume mapping via hidden Markov methods. *IEEE Transactions on Systems, Man and Cybernetics, Part B: Cybernetics, 33*(6), 850–863.

Farrell, J. A., Pang, S., & Li, W. (2005). Chemical plume tracing via an autonomous underwater vehicle. *IEEE Journal of Oceanic Engineering, 30*(2), 428–442.

Formanowicz, D., Kozak, A., Glowacki, T., Radom, M., & Formanowicz, P. (2013). Hemojuvelin-hepcidin axis modeled and analyzed using Petri nets. *Journal of Biomedical Informatics, 46*(6), 1030–1043.

Gardiner, J. M., & Atema, J. (2010). The function of bilateral odor arrival time differences in olfactory orientation of sharks. *Current Biology, 20*(13), 1187–1191.

Grasso, F. W., & Atema, J. (2002). Integration of flow and chemical sensing for guidance of autonomous marine robots in turbulent flows. *Environmental Fluid Mechanics, 2*(1), 95–114.

Hamp, Q., Zhang, R., Chen, L., Gorgis, O., Ostertag, T., Loschonsky, M., et al. (2014). New technologies for the search of trapped victims. *Ad Hoc Networks, 13*, 69–82 (Special issue).

Harvey, D. J., Lu, Tien.-Fu., & Keller, M. A. (2008). Comparing insect-inspired chemical plume tracking algorithms using a mobile robot. *IEEE Transactions on Robotics, 24*(2), 307–317.

Jaques, P. A., Seffrin, H., Rubi, G., Morais, F. D., Ghilardi, C., Bittencourt, L. L., et al. (2013). Rule-based expert systems to support step-by-step guidance in algebraic problem solving: The case of the tutor PAT2Math. *Expert Systems with Applications, 40*(14,15), 5456–5465.

Jiang, Z. B. (2004). *Petri nets and applications for manufacturing system modeling and control*. Peking: China Machine Press (pp. 39–44).

Kamio, M., Grimes, T. V., Hutchins, M. H., Dam, R. V., & Derby, C. D. (2010). The purple pigment aplysioviolin in sea hare ink deters predatory blue crabs through their chemical senses. *Animal Behaviour, 80*(1), 89–100.

Lee, J. S. (2011). A filtering agent scheme to remote control of industrial processes using Petri nets. *Expert Systems with Applications, 38*(12), 15310–15315.

Li, W., Farrell, J. A., & Cardé, R. T. (2001). Tracking of fluid-advected odor plumes: Strategies inspired by insect orientation to pheromone. *Adaptive Behavior, 9*(3–4), 143–170.

Li, W., Farrell, J. A., & Pang, S. (2006). Moth-inspired chemical plume tracing on an autonomous underwater vehicle. *IEEE Transactions on Robotics, 22*(2), 292–307.

Liu, Z., Li, H., & Zhou, P. (2011). Towards timed fuzzy Petri net algorithms for chemical abnormality monitoring. *Expert Systems with Applications, 38*(8), 9724–9728.

Louis, M., Huber, T., Benton, R., Sakmar, T. P., & Vosshall, L. B. (2008). Bilateral olfactory sensory input enhances chemotaxis behavior. *Nature Neuroscience, 11*(2), 187–199.

Lu, T. F. (2013). Indoor odour source localisation using robot: Initial location and surge distance matter? *Robotics and Autonomous Systems, 61*(6), 637–647.

Mansour, M. M., Wahab, M. A. A., & Soliman, W. M. (2013). Petri nets for fault diagnosis of large power generation station. *Ain Shams Engineering Journal, 4*(4), 831–842.

Mayo, M., & Beretta, L. (2011). Modelling epistasis in genetic disease using Petri nets, evolutionary computation and frequent itemset mining. *Expert Systems with Applications, 38*(4), 4006–4013.

Moriizumi, T. & Ishida, H. (2002). Robotic systems to track chemical plumes. In *Proceedings of the 2002 conference on optoelectronic and microelectronic materials and devices* (pp. 537–540).

Porter, J., Craven, B., Khan, R. M., et al. (2007). Mechanisms of scent-tracking in humans. *Nature Neuroscience, 10*(1), 27–29.

Putman, N. F., Lohmann, K. J., Putman, E. M., Quinn, T. P., Klimley, A. P., & Noakes, D. L. G. (2013). Evidence for geomagnetic imprinting as a homing mechanism in pacific salmon. *Current Biology, 23*(4), 312–316.

Rajan, R., Clement, J. P., & Bhalla, U. S. (2006). Rats smell in stereo. *Science, 311*(5761), 666–670.

Renganathan, K., & Bhaskar, V. (2013). Modeling, analysis and performance evaluation for fault diagnosis and fault tolerant control in bottle-filling plant modeled using hybrid Petri nets. *Applied Mathematical Modelling, 37*(7), 4842–4859.

Rozas, R., Morales, J. & Vega, D. (1991). Artificial smell detection for robotic navigation. In *Proceedings of the fifth international conference on advanced robotics (91 ICAR)* (pp. 1730–1733).

Russell, R. A. (2006). Tracking chemical plumes in 3-dimensions. In *Proceedings of the IEEE international conference on robotics and biomimetics (06 ROBIO)* (pp. 31–36).

Sandini, G., Lucarini, G. & Varoli, M. (1993). Gradient driven self-organizing systems. In *Proceedings of the 1993 IEEE/RSJ international conference on intelligent robots and systems* (pp. 429–432).

Shuo, Pang., & Farrell, Jay A. (2006). Chemical plume source localization. *IEEE Transactions on Systems, Man and Cybernetics, Part B: Cybernetics, 36*(5), 1068–1080.

Steck, K., Knaden, M., & Hansson, B. S. (2010). Do desert ants smell the scenery in stereo? *Animal Behaviour, 79*(4), 939–945.

Takasaki, T., Namiki, S., & Kanzaki, R. (2012). Use of bilateral information to determine the walking direction during orientation to a pheromone source in the silkmoth Bombyx mori. *Journal of Comparative Physiology A, 198*(4), 295–307.

Tan, L. (2007). *Digital signal processing: Fundamentals and applications*. Burlington, MA, USA: Academic Press (pp. 13–16).

Tüysüz, F., & Kahraman, C. (2010). Modeling a flexible manufacturing cell using stochastic Petri nets with fuzzy parameters. *Expert Systems with Applications, 37*(5), 3910–3920.

Vidal, J. C., Lama, M., Diaz-Hermida, F., & Bugarin, A. (2013). A Petri net model for changing units of learning in runtime. *Knowledge-Based Systems, 41*(3), 26–42.
Wang, J. H. (2003). *Computer control techniques*. Peking: Higher Education Press (pp. 67–201). .
Wang, W. M., Peng, X., Zhu, G. N., Hu, J., & Peng, Y. H. (2014). Dynamic representation of fuzzy knowledge based on fuzzy Petri net and genetic-particle swarm optimization. *Expert Systems with Applications, 41*(4), 1369–1376.
Webster, D. R. (2007). *Trace chemical sensing of explosives*. Hoboken, NJ: Wiley-Interscience, John Wiley & Sons (pp. 109–129).
Webster, D. R., Volyanskyy, K. Y., & Weissburg, M. J. (2012). Bioinspired algorithm for autonomous sensor-driven guidance in turbulent chemical plumes. *Bioinspiration & Biomimetics, 7*(3), 23–34.
Yang, B. S., Jeong, S. K., Oh, Y. M., & Tan, A. C. C. (2004). Case-based reasoning system with Petri nets for induction motor fault diagnosis. *Expert Systems with Applications, 27*(2), 301–311.
Yu, D., & Frincke, D. (2007). Improving the quality of alerts and predicting intruder's next goal hidden colored Petri-net. *Computer Networks, 51*(3), 632–654.
Yuan, C. Y. (2005). *Petri net theory and applications*. Peking: Publishing House of Electronics Industry (pp. 1–96).
Zhang, M. S., Cui, G. X., & Xu, C. X. (2005). *Theory and modeling of turbulence*. Peking: Tsinghua University Press (pp. 1–23).
Zhou, Q., Huang, G. H., & Chan, C. W. (2004). Development of an intelligent decision support system for air pollution control at coal-fired power plants. *Expert Systems with Applications, 26*(3), 335–356.